Photochemistry of Ozone–Water Complex in Cryogenic Neon, Argon and Krypton Matrices.

ARTICLE *in* THE JOURNAL OF PHYSICAL CHEMISTRY A · NOVEMBER 2013

Impact Factor: 2.69 · DOI: 10.1021/jp4094723 · Source: PubMed

THE JOURNAL OF PHYSICAL CHEMISTRY A

Article

pubs.acs.org/JPCA

Photochemistry of the Ozone−Water Complex in Cryogenic Neon, Argon, and Krypton Matrixes

Masashi Tsuge,*[†,§] Kazuhide Tsuji,[‡] Akio Kawai,[†] and Kazuhiko Shibuya*[†]

[†]Department of Chemistry, Graduate School of Science and Engineering, Tokyo Institute of Technology, 2-12-1 H89 Ohokayama, Meguro-ku, Tokyo 152-8551, Japan

[‡]Gunma National College of Technology, 580 Toriba-machi, Maebashi, Gunma 371-8530, Japan

ABSTRACT: The photochemistry of ozone−water complexes and the wavelength dependence of the reactions were studied by matrix isolation FTIR spectrometry in neon, argon, and krypton matrixes. Hydrogen peroxide was formed upon the irradiation of UV light below 355 nm. Quantitative analyses of the reactant and product were performed to evaluate the matrix cage effect of the photoreaction. In argon and krypton matrixes, a bimolecular $O(^1D) + H_2O \rightarrow H_2O_2$ reaction was found to occur to form hydrogen peroxide, where the $O(^1D)$ atom generated by the photolysis of ozone diffused in the cryogenic solids to encounter water. In a neon matrix, hydrogen peroxide was generated through intracage photoreaction of the ozone−water complex, indicating that a neon matrix medium is most appropriate to study the photochemistry of the ozone−water complex.

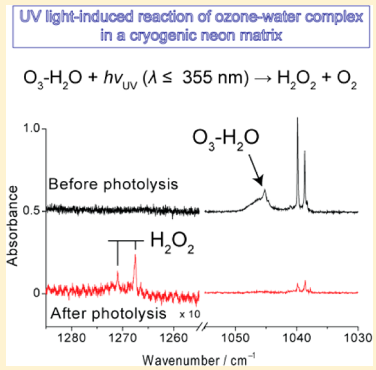

INTRODUCTION

The photochemical hydroxyl radical (OH) generation from ozone plays an important role in tropospheric chemistry and works as a measure to control the oxidation ability of the atmosphere.[1] An excited-state oxygen atom $O(^1D)$, which is formed by photodissociation of ozone molecule, reacts with water vapor to form the OH radical

$$O(^1D) + H_2O(gas) \rightarrow 2OH \quad (1)$$

The $O(^1D)$ atom could be produced from the spin-allowed fragmentation reaction of

$$O_3 + h\nu\ (\lambda \leq 310\ nm) \rightarrow O(^1D) + O_2(a^1\Delta_g) \quad (2)$$

and the spin-forbidden fragmentation reaction of

$$O_3 + h\nu\ (\lambda \leq 411\ nm) \rightarrow O(^1D) + O_2(X^3\Sigma_g^-) \quad (3)$$

where the wavelength regions given in parentheses indicate the threshold wavelengths for the corresponding fragmentation channels. The important quantities of the atmospheric interest in O_3 photochemistry are the $O(^1D)$ yield and its wavelength dependence. The recommended values are reported in a series of NASA Jet Propulsion Laboratory (NASA/JPL) publications.[2,3] In the earlier recommendation,[2] the $O(^1D)$ production occurred only via reaction 2. Later in the 1990s, non-negligible $O(^1D)$ yields were recognized in the photolysis at wavelengths longer than 310 nm. For example, Silvente et al. reported the $O(^1D)$ yield of ∼0.05 at ∼336 nm,[4] clearly above the threshold wavelength of reaction 2. Other experimental results are summarized in the IUPAC Summary of Reactions and Preferred Rate Data.[5] The most recent NASA/JPL recommendation value for the $O(^1D)$ yield in the wavelength range of 329−340 nm is 0.08 ± 0.04, independent of temperature, and for $\lambda > 340$ nm, the quantum yield may be nonzero, but no recommendation has been made.[3] Bauer et al. reported a constant quantum yield of 0.06 between 325 and 375 nm.[6] The UV light below 340 nm is thought to be important in the $O(^1D)$ production from the O_3 monomer in the actual atmosphere because the absorption coefficient of the O_3 monomer above 340 nm is extremely small.[7]

The ozone−water complex has received considerable attention for 2 decades.[7−20] Due to the ubiquitous existence of water and atmospheric importance of O_3, the characterization of this complex and the evaluation of its atmospheric impact are required. We have reported the infrared (IR) spectrum of the ozone−water complex isolated in a neon matrix.[19] On the basis of the spectroscopic and computational results, the atmospheric abundance of the ozone−water complex was calculated to be 2.0 ppt (∼5×10^7 molecules cm^{-3}) under the conditions of a temperature of 298 K, pressure of 1 atm, tropospheric ozone concentration of 50 ppb, and relative humidity of 50%. According to the most recent estimation by Anglada et al.,[20] the concentration of the ozone−water complex is up to 5.74×10^8 molecules cm^{-3} in very hot and humid conditions at the ground level, being 1 order of magnitude larger than our estimate.

Although the abundance of the ozone−water complex seems to be negligibly small, the ozone−water complex will play a partial role if the hydroxyl radical yield from the complex is high. Hurwitz and Naaman reported that the quantum yield of

Received: September 23, 2013
Revised: October 28, 2013
Published: November 19, 2013

the OH radical through the 355 nm photolysis of the ozone−water complex is 1% of that of 266 nm photolysis, although the absorption coefficient of the ozone monomer at 355 nm is 0.01% of that of 266 nm.[8] These values mean that upon the water complex formation, the product of the absorption coefficient and $O(^1D)$ quantum yield increases by 2 orders of magnitude. This result implies that the OH radical might be produced efficiently through the photolysis of the ozone−water complex.[9] Frost and Vaida proposed that 1−15% of OH radical in the troposphere is produced from the ozone−water complex under the assumption that the OH radical could be produced by 260−700 nm light.[11] They considered OH radical formation upon a longer wavelength (λ > 411 nm) irradiation, though the $O(^1D)$ atom is not generated energetically. After all, experimental studies on the wavelength dependence of the photochemistry of the ozone−water complex are necessary to evaluate the photochemical OH radical generation.

The matrix isolation FTIR method is one of the powerful means to study the photochemistry of weakly bound complexes because it can accumulate a large amount of complex and monitor reactants and photoproducts simultaneously. The photochemistry of the ozone monomer and its dimer in cryogenic matrixes has been investigated well.[21,22] On the other hand, only one paper has been reported on the photochemistry of the ozone−water complex in cryogenic matrixes. Schriver et al. prepared the ozone−water complex in an argon matrix and studied the photochemistry of the complex in the UV region below 310 nm.[16] Photodecomposition of ozone monomer and the ozone−water complex and the formation of hydrogen peroxide were observed. They reported that no photochemistry was observed upon the λ > 310 nm irradiation. This result seems to conflict with the observation of OH radical in the 355 nm photolysis of the ozone−water complex in a molecular beam.[8]

In this paper, the ozone−water complex in cryogenic matrixes was revisited to study the photochemistry and the cage effect in three matrix media of neon, argon, and krypton. For UV irradiation, 253.7, 313, 355, and 365 nm were selected for photolysis. In the wavelength region excluding 253.7 nm, the spin-forbidden reaction 3 is thought to be important. The visible 632.8 nm irradiation was also performed to check whether the OH radical is produced or not by visible light (λ > 411 nm). The 632.8 nm light corresponds to visible Chappuis absorption bands of ozone.

EXPERIMENT

Ozone was prepared in a silica gel trap at ∼200 K by removing oxygen from an ozone/oxygen mixture produced by a commercial ozonizer. Mixtures of O_3/H_2O/Rg (Rg = Ne, Ar, and Kr) and $O_3/H_2{}^{18}O$/Ne were prepared in glass bulbs by standard manometric techniques. Gas samples were deposited onto a CsI substrate that was cooled by a closed-cycle helium refrigerator (Iwatani, CryoMini). The deposition temperatures for neon, argon, and krypton samples were ∼6, 20, and 35 K, respectively. The IR spectra with 0.0625 cm^{-1} resolution were recorded by using a FTIR spectrometer (JEOL, SPX200) equipped with a liquid-nitrogen-cooled MCT detector.

The 355 nm photodissociation was carried out using the third-harmonic Nd:YAG lasers (Continuum, Surelite and Coherent, AVIA X). An ultrahigh pressure mercury lamp (USHIO, USH-500SC) with appropriate interference filters was used to select 313 or 365 nm. A low-pressure mercury lamp (Spectronics, Spectroline) with a cutoff filter (Corning) was used for 253.7 nm light. A He−Ne laser (JDS Uniphase, NOVETTE) was used for 632.8 nm. All lights were introduced into a matrix chamber through a quartz window.

Quantum chemical calculations were performed using the Gaussian 03 package.[23] Geometry optimization and vibrational frequency analysis were performed at the QCISD/6-311++G(d,p) level of theory.

RESULTS AND DISCUSSION

IR Absorption Spectra of the Ozone Monomer and Ozone−Water Complex. The photoreactions of the ozone monomer and ozone−water complex were monitored in a spectral region around the fundamental ν_3 frequency of ozone. Figure 1 shows the IR spectra of the ozone monomer and ozone−water complex isolated in (a) neon, (b) argon, and (c) krypton matrixes. The asymmetric stretching ν_3 band of the ozone monomer has a doublet structure due to the matrix site effect. The stronger and weaker bands of the ozone monomer are assigned to bands due to the stable and metastable sites, respectively, in rare gas solids.[24] As assigned in our previous paper,[19] the ozone−water complex band in neon appears at around 1045 cm^{-1} (∼6 cm^{-1} blue-shifted from monomer). In argon, the ozone−water band was observed at 1037.5 cm^{-1}

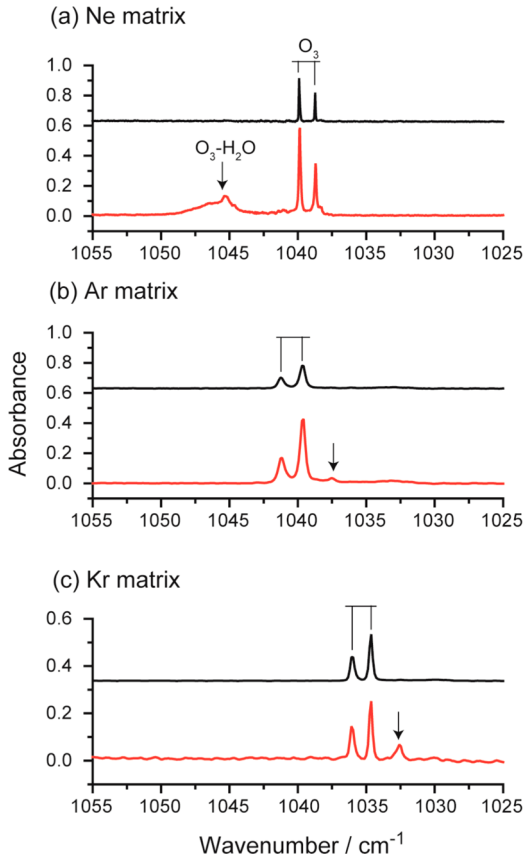

Figure 1. IR absorption spectra of ozone monomer and the ozone−water complex in (a) neon, (b) argon, and (c) krypton matrixes. The matrix samples were prepared from O_3/Ne = 1/4000, O_3/H_2O/Ne = 1/5/4000, O_3/Ar = 1/1500, O_3/H_2O/Ar = 1/2.5/1500, O_3/Kr = 1/8000, and O_3/H_2O/Kr = 1/1/8000. The upper and lower traces were recorded for the matrixes without and with water, respectively. Arrows indicate the absorption peaks due to the ozone−water complex in the corresponding cryogenic matrixes.

dx.doi.org/10.1021/jp4094723 | J. Phys. Chem. A 2013, 117, 13105−13111

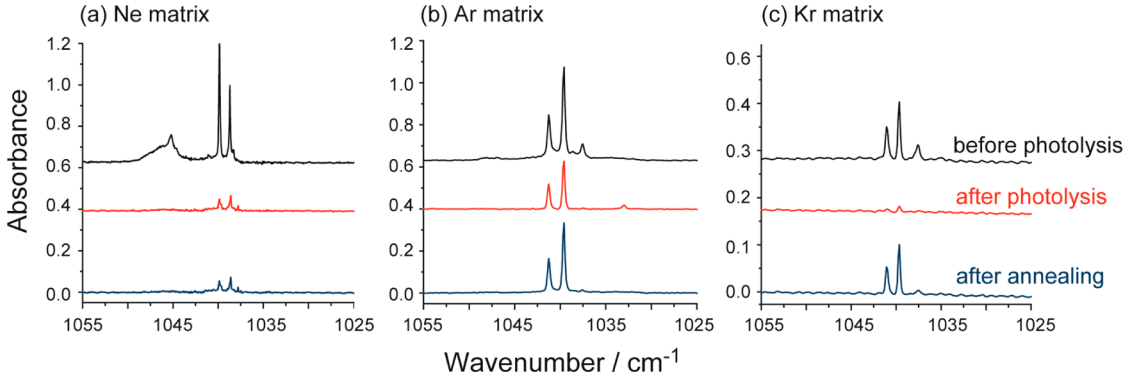

Figure 2. Spectral change upon UV irradiation and subsequent annealing. The top and middle traces were recorded before and after the 355 nm irradiation (5−10 mJ/pulse, 10 Hz), respectively. The irradiation time for neon, argon, and krypton matrixes was about 100, 80, and 24 h, respectively. The bottom trace was recorded after the subsequent annealing of the UV-light-irradiated matrix sample shown in the middle trace. Annealing temperatures were 10, 30, and 35 K for neon, argon, and krypton matrixes, respectively.

(2.1 cm^{-1} red-shifted from monomer). Ozone dimer bands at 1037.8 and 1045.0 cm^{-1} were not observed under our experimental conditions.[22] Although Schriver et al. reported the ozone−water complex band to lie at 1046 cm^{-1},[16] this band did not appear in our measurement (Figure 1b) but was observed only for the $O_3/H_2O/Ar$ sample with excess water. Therefore, we reassigned the 1046 cm^{-1} band to the $O_3-(H_2O)_n$ ($n \geq 2$) complexes. In krypton (Figure 1c), the ozone−water complex was observed at 1032.6 cm^{-1} (2.0 cm^{-1} red-shifted from monomer).

The ozone−water band is blue-shifted from the ozone monomer band in neon, while the complex bands are red-shifted from the monomer bands in argon and krypton. It is of note that the stable site bands of the ozone monomer appear at the blue and red sides of the corresponding metastable bands in neon and argon (or krypton), respectively. Brosset et al. attributed this interesting observation to the difference in the matrix structure,[24,25] which might be one plausible explanation similarly for the matrix shift difference of the ozone−water complex. Another possible explanation would be due to the existence of different conformers of the ozone−water complex. Theoretical studies by Kumar and Sathyamurthy predict that "cis" and "side" conformers show a red shift of the ν_3 mode.[26] For further understanding of this anomalous shift, intensive experimental and theoretical investigations are needed and are beyond the scope of this paper. We assume that the different conformers undergo an identical photoreaction, though the conformation-dependent chemical reactions are known for a few cases.[27−29] As will be discussed below, the photoreaction of the ozone−water complex in cryogenic matrixes can be regarded as a process taking place not within one complex but inside one matrix cage. In the subsequent section, the photochemistry of the ozone−water complex in neon, argon, and krypton matrixes is discussed on the basis of the IR assignment described above.

Spectral Changes upon UV Irradiation and Subsequent Annealing. Figure 2a shows the spectral change of the $O_3/H_2O/Ne$ matrix upon 355 nm light irradiation and the subsequent annealing. Both the bands due to the ozone monomer and ozone−water complex decrease by the UV irradiation but do not increase after the subsequent annealing at 10 K for 1 h. These observations in a neon matrix imply that the UV photolysis of ozone and ozone−water takes place, but ozone is not regenerated after the subsequent annealing at 10 K. Thus, oxygen atoms trapped in a neon matrix are not likely to migrate at 10 K.

In the $O_3/H_2O/Ar$ matrix, as illustrated in Figure 2b, the ozone−water complex (1037.5 cm^{-1}) disappears upon the UV irradiation, while the ozone monomer bands (1041.1 and 1039.6 cm^{-1}) slightly decrease in intensity. The ozone monomer recovers upon the subsequent annealing at 30 K. It should be noted that the $O(^3P)-O_3$ complex appears at 1033 cm^{-1} after the UV irradiation[21] but disappears after the subsequent annealing at 30 K. Oxygen atoms trapped in an argon matrix seem to migrate to regenerate ozone at 30 K. Because the long-range mobility of the oxygen atom is restricted in an argon matrix,[30] the regeneration of ozone at 30 K would be connected with the local mobility of oxygen atoms, that is, an oxygen atom in the vicinity of an O_2 molecule is responsible for the regeneration of ozone.

Figure 2c shows the results obtained for the $O_3/H_2O/Kr$ matrix. Both the ozone monomer and ozone−water complex disappear almost entirely upon the UV irradiation. Almost all ozone monomer regenerates after the subsequent annealing at 35 K, while the recovery of the ozone−water complex is about 30% of the deposited amount. Thermal annealing above 25 K activates extensive mobility of oxygen atoms in solid krypton,[27,31] and oxygen atoms react with O_2 or the O_2-H_2O complex to regenerate ozone monomer or the ozone−water complex. A residual 70% of the initially prepared ozone−water complex is thought to be consumed to produce hydrogen peroxide, as discussed below.

The decrease of ozone monomer upon UV irradiation will be presumably due to the photodecomposition into O_2 and an O atom. The nascent O atoms will stay in the parent cage to recover the ozone by a reaction of $O_2 + O(^3P) \rightarrow O_3$ or exit the cage to travel in the rare gas solid, which results in the bleaching of ozone monomer.

Photochemical Formation of Hydrogen Peroxide. The middle and bottom traces of Figure 3 show the IR spectra of the photoproducts recorded after the 355 nm irradiation of $^{16}O_3/H_2{}^{16}O/Ne$ and $^{16}O_3/H_2{}^{18}O/Ne$ matrixes, respectively. Two product bands at 1267.5 and 1270.0 cm^{-1} (middle trace) are assigned to the ν_6 mode of the hydrogen peroxide monomer ($H^{16}O^{16}OH$).[32] The weak product bands observed at 3609 and 3619 cm^{-1} may originate from the ν_5 mode of $H^{16}O^{16}OH$.[32] The experimental result for the $^{16}O_3/H_2{}^{18}O/Ne$ matrix presents the product bands, which are red-shifted by about 2 cm^{-1} to 1265.0 and 1268.3 cm^{-1}, together with weaker impurity $H^{16}O^{16}OH$ bands at 1267.5 and 1270.0 cm^{-1}. These 1265.0 and 1268.3 cm^{-1} bands are assigned to $H^{18}O^{16}OH$ based on the frequency calculation of hydrogen peroxide isotopologues at the QCISD/6-311++G(d,p) level of theory. The calculation

dx.doi.org/10.1021/jp4094723 | J. Phys. Chem. A 2013, 117, 13105−13111

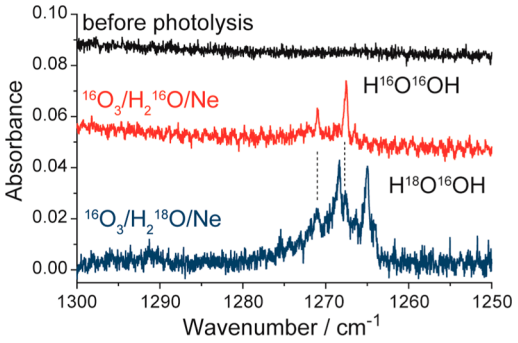

Figure 3. IR absorption spectra of hydrogen peroxide photochemically generated in a neon matrix. The top trace was obtained before UV irradiation. The middle and bottom traces were recorded after the 355 nm irradiation of matrixes made from $^{16}O_3/H_2{}^{16}O/Ne$ = 1/5/4000 and $^{16}O_3/H_2{}^{18}O/Ne$ =1/5/4000 samples, respectively.

indicates that the frequency in the ν_6 fundamental of $H^{18}O^{16}OH$ shifts by −3.2 cm^{-1} from that of $H^{16}O^{16}OH$, which reasonably agrees with the experimental result. Therefore, the isotopic substitution experiment using $H_2{}^{18}O$ supports that hydrogen peroxide is photochemically generated by the UV irradiation of the ozone−water complex in a neon matrix.

As shown in Figure 4 for the argon matrix, the water−hydrogen peroxide complex $(H_2O_2{-}H_2O)$[33] was observed in

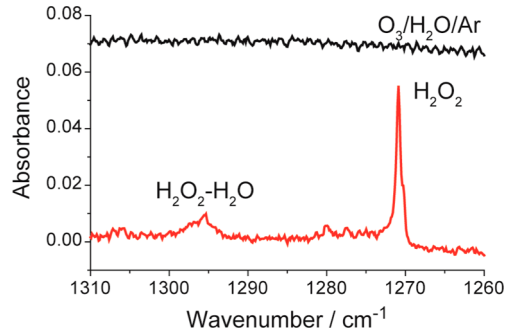

Figure 4. IR absorption spectrum of hydrogen peroxide photochemically generated in an argon matrix. The upper and lower traces were recorded before and after the 355 nm irradiation of the matrix made from the $^{16}O_3/H_2{}^{16}O/Ar$ = 1/2.5/1500 sample.

addition to the hydrogen peroxide monomer as the photochemical product. The formation of $H_2O_2{-}H_2O$ was also observed in a krypton matrix but not in a neon matrix. The photochemical formation of the $H_2O_2{-}H_2O$ is presumably due to the reaction between $(H_2O)_2$ and the $O(^1D)$ atom, where $O(^1D)$ will be generated from the UV photolysis of ozone monomer and probably the ozone−water complex

$$O(^1D) + (H_2O)_2 \rightarrow H_2O_2{-}H_2O \quad (4)$$

It should be noted that the $O_3{-}(H_2O)_2$ complex, which in principle can generate the $H_2O_2{-}H_2O$ complex, was not identified in our experiments (Figure 1). Hydrogen peroxide monomer can be formed by the following two reactions

$$O(^1D) + H_2O \rightarrow H_2O_2 \quad (5)$$

and

$$O_3{-}H_2O + h\nu \rightarrow \{O_2 + O(^1D) + H_2O\} \rightarrow O_2 + H_2O_2 \quad (6)$$

Here, the curly brackets denote species trapped in a matrix cage. Reaction 5 is similar to reaction 4, and reaction 6 denotes the photochemical formation of hydrogen peroxide within a single cage. In an $O_3/H_2O/Ne$ matrix, $H_2O_2{-}H_2O$ was not observed to be formed, though a considerable amount of $(H_2O)_2$ was observed similarly in $O_3/H_2O/Ar$ and $O_3/H_2O/Kr$ matrixes. Furthermore, noticeable changes upon photolysis were not observed for water monomer bands in a neon matrix, while the decrease of water monomer and dimer bands was seen in argon and krypton matrixes, to some extent. These results suggest that hydrogen peroxide in the $O_3/H_2O/Ne$ system is photochemically generated within a matrix cage, through reaction 6, where the ozone−water complex is isolated. The matrix effect of the $O(^1D)$ mobility in argon and xenon solids has been studied by Ning et al.,[34,35] and the travel distance of $O(^1D)$ in xenon is twice as long as that in argon; the $O(^1D)$ mobility is better facilitated in xenon than in argon because the solid structure is more porous in xenon than in argon. Thus, one can expect less travel of the $O(^1D)$ atom in neon than in argon, which agrees with our experimental results described above.

Figure 5 shows the kinetic decay of the ozone−water complex obtained by varying the laser pulse energy from 17 to 50 μJ

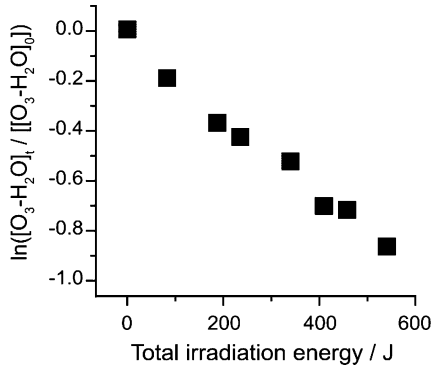

Figure 5. Kinetic decay of the ozone−water complex upon the 355 nm irradiation in a neon matrix. The horizontal axis corresponds to total irradiation energy obtained for the product of the laser pulse energy (17−50 μJ/pulse) and laser shot number (~2 × 10^7 shots).

in an $O_3/H_2O/Ne$ system. The horizontal axis of this plot corresponds to the product of the pulse energy and laser shot number, that is, the total irradiation energy. The linear relation suggests that the photolysis of the ozone−water complex at 355 nm is dominated by a single-photon absorption in the pulse energy range below 50 μJ. When the pulse energy became higher than 10 mJ, the kinetic decay curves showed a characteristic behavior for two photon processes.

Formation Yield of Hydrogen Peroxide. The formation yield of hydrogen peroxide is expressed as

$$Y_{H_2O_2} = \frac{[H_2O_2]_t}{[O_3{-}H_2O]_0 - [O_3{-}H_2O]_t} \quad (7)$$

where $[X]_0$ and $[X]_t$ are relative abundances of species X before and after the photolysis, respectively. The relative abundances were calculated from the experimental IR intensity and calculated integrated absorption coefficient. The experimental IR intensity was determined by integrating the area of the corresponding IR peak. The integrated absorption coefficients for the ozone ν_3 vibration within the ozone−water complex and

dx.doi.org/10.1021/jp4094723 | J. Phys. Chem. A 2013, 117, 13105−13111

Table 1. Relative Abundances of the O_3–H_2O Complex and H_2O_2 before and after 355 nm Photolysis (~5 mJ/pulse)[a]

	$[O_3–H_2O]_0$[b]	$[O_3–H_2O]_t$[b]	$[H_2O_2]_t$[b]	$Y_{H_2O_2}$[c]
neon (t > 100 h)	3.1×10^{-5}	0.1×10^{-5}	3.0×10^{-5}	1.0
	(1.5×10^{-2})[d]	(5×10^{-5})[d]	(3.0×10^{-3})[d]	
argon (t = 25 h)	9.0×10^{-5}	2.8×10^{-5}	5.6×10^{-4}[e]	9.0[e]
	(4.5×10^{-2})[d]	(1.4×10^{-2})[d]	(5.5×10^{-2})[d]	
krypton (t = 6 h)	4.0×10^{-5}	1.6×10^{-5}	9.9×10^{-5}[e]	4.1[e]
	(2.0×10^{-2})[d]	(0.8×10^{-2})[d]	(9.8×10^{-3})[d]	

[a]Results of quantitative analyses are listed for matrix samples prepared from the gas mixtures of $O_3/H_2O/Ne$ = 1/1.5/1000, $O_3/H_2O/Ar$ = 1/2.5/1000, and $O_3/H_2O/Kr$ = 1/1/8000. [b]The symbols of $[X]_0$ and $[X]_t$ denote the relative abundances of species X before and after photolysis, respectively, which are calculated by dividing experimental IR intensities (integrated area) by calculated integrated absorption coefficients of 498.5 (O_3–H_2O) and 98.6 (H_2O_2) km mol^{-1}. [c]Defined as shown in eq 7. [d]Experimental IR intensities are shown in parentheses. [e]In argon and krypton matrixes, the $[H_2O_2]_t$ amounts were dependent on $[H_2O]_0$, and the $Y_{H_2O_2}$ values were larger than unity (see text).

ozone monomer were calculated to be 498.5 and 396.2 km mol^{-1}, respectively, at the QCISD/6-311++G(d,p) level of theory. For the hydrogen peroxide monomer, the integrated absorption coefficient of the ν_6 mode was calculated to be 98.6 km mol^{-1}. By using the calculated integrated absorption coefficients (498.5 and 98.6 km mol^{-1} for the ozone–water complex and hydrogen peroxide, respectively), the hydrogen peroxide formation yield ($Y_{H_2O_2}$) upon the 355 nm irradiation in a neon matrix is estimated to be almost unity (Table 1). On the other hand, in argon and krypton matrixes, the $Y_{H_2O_2}$ values are calculated to be as large as 9 and 4, respectively. The experimental $Y_{H_2O_2}$ values that are much larger than unity mean that, in $O_3/H_2O/Ar$ and $O_3/H_2O/Kr$ systems, the photoproduct of hydrogen peroxide is generated mainly through the diffusion-controlled reaction between $O(^1D)$ and H_2O, reaction 5, and rather additionally by the UV photolysis of the ozone–water complex, reaction 6.

If hydrogen peroxide in an argon matrix is generated only by reaction 5 and we assume the relative amounts of $[O_3–H_2O]/[O_3]/[H_2O]$ are 0.1:1:2.5, the water monomer is expected to decrease by 30% in amount, where the $[O_3–H_2O]/[O_3]$ ratio is estimated from the integrated band intensities observed and the $[O_3]/[H_2O]$ ratio is proportional to the mixing ratio of the samples. However, the water monomer did not decrease by such a large amount in an argon matrix upon the photoirradiation. One possibility is that the relative amounts of O_3 and H_2O in a deposited matrix is different from that in a sample bulb. Indeed, in the matrix sample prepared from $O_3/H_2O/Ar$ = 1/2.5/1500, the relative amount of O_3 and H_2O is estimated from the integrated intensities of O_3 ν_3 and H_2O ν_2 bands to be $[O_3]/[H_2O]$ = 1:20. This estimate implies that the decrease of the H_2O monomer in an argon matrix due to reaction 5 may be up to 5%, which is consistent with our observation. The $Y_{H_2O_2}$ values obtained for argon and krypton matrixes varied depending on the amount of water and were found to be larger than unity due to reaction 5. It should be noted that the $Y_{H_2O_2}$ values derived for the neon matrix remained constant around unity, which would reflect the hydrogen peroxide formation by the UV photolysis of the ozone–water complex.

Wavelength Dependence of Photoreaction of an $O_3/H_2O/Ne$ Matrix. Ultraviolet irradiation at 365, 355, 313, and 253.7 nm was performed for $O_3/H_2O/Ne$ samples. The 365 nm irradiations lead to the decomposition of not ozone and ozone–water but ozone dimer. The decomposition of the ozone dimer is reported to occur through the reaction[21]

$$(O_3)_2 + h\nu \rightarrow \{O_2 + O + O_3\} \rightarrow 3O_2 \quad (8)$$

The absorption coefficient at 365 nm is extremely low, and the observation of ozone dimer decomposition required sufficient irradiation time.

Recently, Jin et al. have reported the UV absorption cross sections of the ozone–water complex, and they did not observe any absorption at 351.8 nm,[18] which seems to conflict with our observation of the photolysis of the ozone–water complex at 355 nm. Possibly, this difference of statement originates from the difference in two experimental detection limits. In fact, quite a long irradiation time was required to detect the photoreaction of the $O_3/H_2O/Ne$ matrix at 355 nm; ~1×10^7 pulses with the pulse energy of ~5 mJ were needed to photolyze the ozone–water complex up to 90%.

By the 313 and 253.7 nm irradiations, the decomposition of the ozone monomer and ozone–water complex and the formation of hydrogen peroxide were observed. Though Schriver et al. observed the OH and HO_2 radicals by λ < 310 nm irradiation in an argon matrix,[16] we observed neither OH nor HO_2 radicals in a neon matrix with all of the wavelength irradiations employed (253.7, 313, 355, and 365 nm).

The visible light irradiation at 632.8 nm did not lead to any changes in the band intensity of the ozone–water complex (and the ozone monomer as well) presumably due to the photolysis to generate the $O(^3P)$ atom followed by a recombination to regenerate ozone in a matrix cage. The occurrence of such intracluster photolysis/recombination reactions is recognized by red-light-induced photoreactions reported for an ozone–dimethyl sulfide complex[36] and As_4–O_3 complex.[37]

Reaction Mechanism for Hydrogen Peroxide Formation. As discussed above, hydrogen peroxide in a neon matrix is generated from the ozone–water complex, while significant contribution from reaction 5 is obvious in argon and krypton matrixes. Here, we discuss the mechanisms for the formation of hydrogen peroxide within one cage, that is, from the ozone–water complex.

In the analogy from the gas-phase reaction of $O(^1D)$ with H_2O, the following reactions are thought

$$\begin{aligned} O_3–H_2O + h\nu\ (355\text{nm}) &\rightarrow \{O_2 + O(^1D) + H_2O\} \\ &\rightarrow \{O_2 + 2OH\} \\ &\rightarrow O_2 + H_2O_2 \end{aligned} \quad (9)$$

The OH radical might escape the original neon matrix cage, but we did not observe OH in our experiments. Furthermore, if OH radical escapes the cage, one expects the isotope-scrambling reactions between ^{16}OH and ^{18}OH radicals from different

dx.doi.org/10.1021/jp4094723 | J. Phys. Chem. A 2013, 117, 13105–13111

cages, which would result in an equivalent formation of three isotopologues ($H^{16}O^{16}OH$, $H^{16}O^{18}OH$, and $H^{18}O^{18}OH$). Figure 3 shows that $H^{18}O^{16}OH$ is the main isotopologue of the H_2O_2 product, while the amount of $H^{18}O^{18}OH$ is below the detection limit and $H^{16}O^{16}OH$ is formed by the photolysis of $^{16}O_3$/impurity $H_2{}^{16}O$. The 193 nm photolysis of hydrogen peroxide in argon and krypton matrixes is known to produce OH radical and an $H_2O{-}O(^3P)$ complex.[38] The available kinetic energy of the nascent OH radical in the 193 nm photolysis of hydrogen peroxide is about 2 eV, which is sufficient for cage exit. However, the available kinetic energy of OH in the present reaction of $O(^1D) + H_2O \rightarrow 2OH$ is about 0.6 eV, which might be insufficient for cage exit.

In general, two reaction mechanisms will be possible to explain the H_2O_2 formation from a photolytic $O_3{-}H_2O$ system in the solid state; two OH radicals formed in one cage recombine to form H_2O_2 (reaction 9), and the photolytic $O_3{-}H_2O$ complex in the cage produces vibrationally hot H_2O_2 through a direct insertion-type mechanism before OH comes into existence as transient molecular species. In either case of the mechanism, an activated hydrogen peroxide will be stabilized in the cage to form the final product. Sayós et al. have calculated the direct potential energy surface between the $O(^1D) + H_2O$ and H_2O_2,[38] and the activated hydrogen peroxide formed via insertion is proposed to form OH radicals in the gas-phase $O(^1D) + H_2O$ reaction,[39] which corresponds to the insertion-type mechanism in the solid state described above.

CONCLUSIONS

The photochemistry of the ozone–water complex isolated in cryogenic neon, argon, and krypton matrixes was studied. The ν_3 fundamental region of ozone in the FTIR spectra was chosen to monitor the photoreactions of the ozone monomer and ozone–water complex. The UV irradiation at 355, 313, and 253.7 nm induced the decompositions of the ozone monomer and ozone–water complex with the formation of hydrogen peroxide. These reactions were not observed for the 365 and 632.8 nm irradiations. The quantitative analysis of the photolysis of the ozone–water complex and the generation of hydrogen peroxide have revealed that hydrogen peroxide is generated with the quantum yield of almost unity from the 355 nm photolysis of the ozone–water complex in a neon matrix, while in argon and krypton matrixes, hydrogen peroxide is generated dominantly through a diffusion-controlled bimolecular reaction between the $O(^1D)$ atom and water.

AUTHOR INFORMATION

Corresponding Authors

*E-mail: masashi.tsuge@helsinki.fi. Tel: +358-9-19150287. Fax: +358-9-19150279 (M.T.).

*E-mail: kshibuya@chem.titech.ac.jp (K.S.).

Present Address

§M.T.: Department of Chemistry, University of Helsinki, P.O. Box 55, FIN-00014, Finland.

Notes

The authors declare no competing financial interest.

ACKNOWLEDGMENTS

The present work is partly defrayed by the Grant-in-Aid for Scientific Research (No. 17350005) and by the Grant-in-Aid for Scientific Research on Priority Areas (B) (No. 13127202) from the Ministry of Education, Culture, Sports, Science and Technology, Japan.

REFERENCES

(1) Matsumi, Y.; Kawasaki, M. Photolysis of Atmospheric Ozone in the Ultraviolet Region. *Chem. Rev.* **2003**, *103*, 4767–4781.

(2) DeMore, W. B.; Sander, S. P.; Golden, D. M.; Hampson, R. F.; Kurylo, M. J.; Howard, C. J.; Ravishankara, A. R.; Kolb, C. E.; Molina, M. J. *Chemical Kinetics and Photochemical Data for Use in Stratospheric Modeling*, JPL Publication 97-4; NASA Jet Propulsion Laboratory: Pasadena, CA, 1997.

(3) Sander, S. P.; Barker, J. R.; Golden, D. M.; Kurylo, M. J.; Wine, P. H.; Abbatt, J. P. D.; Burkholder, J. B.; Kolb, C. E.; Moortgat, G. K.; Huie, R. E.; Orkin, V. L. *Chemical Kinetics and Photochemical Data for Use in Atmospheric Studies*, JPL Publication 10-6; NASA Jet Propulsion Laboratory: Pasadena, CA, 2011.

(4) Silvente, E.; Richter, R. C.; Zheng, M.; Saltzman, E. S.; Hynes, A. J. Relative Quantum Yields for O^1D Production in the Photolysis of Ozone between 301 and 336 nm: Evidence for the Participation of a Spin-Forbidden Channel. *Chem. Phys. Lett.* **1997**, *264*, 309–315.

(5) Atkinson, R.; Baulch, D. L.; Cox, R. A.; Crowley, J. N.; Hampson, R. F.; Hynes, R. G.; Jenkin, M. E.; Rossi, M. J.; Troe, J. Evaluated Kinetic and Photochemical Data for Atmospheric Chemistry: Volume I — Gas Phase Reactions of Ox, HOx, NOx, and SOx, Species. *Atmos. Chem. Phys.* **2004**, *4*, 1461–1738 ; http://www.atmos-chem-phys.org/acp/4/1461, and http://www.iupac-kinetic.ch.cam.ac.uk/.

(6) Bauer, D.; D'Ottone, L.; Hynes, A. J. O^1D Quantum Yields from O_3 Photolysis in the Near UV Region between 305 and 375 nm. *Phys. Chem. Chem. Phys.* **2000**, *2*, 1421–1424.

(7) Axson, J. L.; Washenfelder, R. A.; Kahan, T. F.; Young, C. J.; Vaida, V.; Brown, S. S. Absolute Ozone Absorption Cross Section in the Huggins Chappuis Minimum (350–470 nm) at 296 K. *Atmos. Chem. Phys.* **2011**, *11*, 11581–11590.

(8) Hurwitz, Y.; Naaman, R. Production of OH by Dissociationg Ozone–Water Complexes at 266 and 355 nm by Reacting O^1D with Water Dimers. *J. Chem. Phys.* **1995**, *102*, 1941–1943.

(9) Staikova, M.; Donaldson, D. J. Water Complexes as Catalysts in Atmospheric Reactions. *Phys. Chem. Earth, Part C* **2001**, *26*, 473–478.

(10) Vaida, V.; Frost, G. J.; Brown, L. A.; Naaman, R.; Hurwitz, Y. Spectroscopy and Photoreactivity in Complex Environments. *Ber. Bunsen-Ges. Phys. Chem.* **1995**, *99*, 371–377.

(11) Frost, G.; Vaida, V. Atmospheric Implications of the Photolysis of the Ozone–Water Weakly-Bound Complex. *J. Geophys. Res.: Atmos.* **1995**, *100*, 18803–18809.

(12) Gillies, J. Z.; Gillies, C. W.; Suenram, R. D.; Lovas, F. J.; Schmidt, T.; Cremer, D. A Mirrowave Spectral and Ab Initio Investigation of $O_3{-}H_2O$. *J. Mol. Spectrosc.* **1991**, *146*, 493–512.

(13) Tachikawa, H.; Abe, S. Spectral Shifts of Ozone Molecule by the Complex Formation with a Water Molecule. *Chem. Phys. Lett.* **2006**, *432*, 409–413.

(14) Tachikawa, H.; Abe, S. Structures and Excitation Energies of Ozone–Water Clusters $O_3(H_2O)_n$ (n=1–4). *Inorg. Chim. Acta* **2005**, *358*, 288–294.

(15) Tachikawa, H.; Abe, S. Ozone–Water 1:1 Complexes $O_3{-}H_2O$: An Ab Initio Study. *Inorg. Chem.* **2003**, *42*, 2188–2190.

(16) Schriver, L.; Barreau, C.; Schriver, A. Infrared Spectroscopic and Photochemical Study of Water–Ozone Complexes in Solid Argon. *Chem. Phys.* **1990**, *140*, 429–438.

(17) King, D. S.; Sauder, D. G.; Casassa, M. P. Cluster Effects in O_3/H_2O Photochemistry: Dynamics of the $O+H_2O \rightarrow 2OH$ Reaction Photoinitiated in the $O_3{\cdot}H_2O$ Dimer. *J. Chem. Phys.* **1994**, *100*, 4200–4210.

(18) Jin, B.; Su, M. N.; Lin, J. J. M. Does Ozone–Water Complex Produce Additional OH Radicals in the Atmosphere? *J. Phys. Chem. A* **2012**, *116*, 12082–12088.

(19) Tsuge, M.; Tsuji, K.; Kawai, A.; Shibuya, K. Infrared Spectroscopy of Ozone–Water Complex in a Neon Matrix. *J. Phys. Chem. A* **2007**, *111*, 3540–3547.

(20) Anglada, J. M.; Hoffman, G. J.; Slipchenko, L. V.; M.Costa,, M.; Ruiz-López, M. F.; Francisco, J. S. The Atmospheric Significance of Water Clusters and Ozone−Water Complexes. *J. Phys. Chem. A* **2013**, *117*, 10381−10396.
(21) Bahou, M.; Schriver-Mazzuoli, L.; Schriver, A. Infrared Spectroscopy and Photochemistry at 266 nm of the Ozone Dimer Trapped in an Argon Matrix. *J. Chem. Phys.* **2001**, *114*, 4045−4052.
(22) Bahou, M.; Schriver-Mazzuoli, L.; Schriver, A. Photolysis at 266 nm of Argon Matrix Isolated Ozone Monomer. *J. Chem. Phys.* **1999**, *110*, 8636−8642.
(23) Frisch, M. J.; Trucks, G. W.; Schlegel, H. B.; Scuseria, G. E.; Robb, M. A.; Cheeseman, J. R.; Montgomery, J. A.; Vreven, T.; Kudin, K. N.; Burant, J. C.; et al. *Gaussian 03*, revision C.01; Gaussian Inc.: Wallingford, CT, 2003.
(24) Brosset, P.; Dahoo, R.; Gauthier-Roy, B.; Abouaf-Maguin, L.; Lakhlifi, A. Analysis of IR Absorption Spectrum of O_3 in Inert Matrices: Spectroscopic Evidence for Two Trapping Sites. *Chem. Phys.* **1993**, *172*, 315−324.
(25) Lakhlifi, A.; Girardet, C.; Dahoo, R.; Brosset, P.; Gauthier-Roy, B.; Abouaf-Maguin, L. Interpretation of the Infrared Spectrum of Ozone Trapped in Inert Matrices. *Chem. Phys.* **1993**, *177*, 31−44.
(26) Kumar, P.; Sathyamurthy, N. An Ab Initio Quantum Chemical Investigation of the Structure and Stability of Ozone−Water Complexes. *Chem. Phys.* **2013**, *415*, 214−221.
(27) Khriachtchev, L.; Domanskaya, A.; Marushkevich, K.; Räsänen, M.; Grigorenko, B.; Ermilov, A.; Andrijchenko, N.; Nemukhin, A. Conformation-Dependent Chemical Reaction of Formic Acid with an Oxygen Atom. *J. Phys. Chem. A* **2009**, *113*, 8143−8146.
(28) Taatjes, C. A.; Welz, O.; Eskola, A. J.; Savee, J. D.; Scheer, A. M.; Shallcross, D. E.; Rotavera, B.; Lee, E. P. F.; Dyke, J. M.; Mok, D. K. W.; et al. Direct Measurements of Conformer-Dependent Reactivity of the Criegee Intermediate CH_3CHOO. *Science* **2013**, *340*, 177−180.
(29) Chang, Y.-P.; Długołęcki, K.; Küpper, J.; Rösch, D.; Wild, D.; Willitsch, S. Specific Chemical Reactivities of Spatially Separated 3-Aminophenol Conformers with Cold Ca^+ Ions. *Science* **2013**, *342*, 98−101.
(30) Khriachtchev, L.; Pettersson, M.; Pehkonen, S.; Isoniemi, E.; Räsänen, M. Low-Temperature Thermoluminescence in Solid Argon: Short-Range Mobility of Atoms. *J. Chem. Phys.* **1999**, *111*, 1650−1657.
(31) Pehkonen, S.; Marushkevich, K.; Khriachtchev, L.; Räsänen, M.; Grigorenko, B. L.; Nemukhin, A. V. Photochemical Synthesis of H_2O_2 from the $H_2O\cdots O(^3P)$ van der Waals Complex: Experimental Observations in Solid Krypton and Theoretical Modeling. *J. Phys. Chem. A* **2007**, *111*, 11444−11449.
(32) Thompson, W. E.; Lugez, C. L.; Jacox, M. E. The Infrared Spectrum of $HOOH^+$ Trapped in Solid Neon. *J. Chem. Phys.* **2012**, *137*, 144305.
(33) Engdahl, A.; Nelander, B. The Structure of the Water−Hydrogen Peroxide Complex. A Matrix Isolation Study. *Phys. Chem. Chem. Phys.* **2000**, *2*, 3967−3970.
(34) Ning, X. J.; Qin, Q. Z. Matrix Effects on the Mobility of Oxygen Atoms in Different States. *J. Chem. Phys.* **2001**, *114*, 9969−9974.
(35) Ning, X. J.; Zhang, L. N.; Chen, M. H.; Qin, Q. Z. Mobility of Oxygen Atoms Generated from Photolysis of O_3 Isolated in Argon Matrices. *J. Chem. Phys.* **2000**, *112*, 386−395.
(36) Wakamatsu, D.; Akai, N.; Kawai, A.; Shibuya, K. Red-Light-Induced Photoreaction of DMS−O_3 Complex in a Cryogenic Neon Matrix. *Chem. Lett.* **2012**, *41*, 252−253.
(37) Andrews, L.; Mielke, Z. Infrared Spectra of the Tetraarsenic-Ozone Reaction and Photolysis Products in Solid Argon. *Inorg. Chem.* **1989**, *28*, 4001−4006.
(38) Sayós, R.; Oliva, C.; González, M. Ab Initio CASPT2//CASSCF Study of the $O(^1D)+H_2O(X\ ^1A_1)$ Reaction. *J. Chem. Phys.* **2001**, *115*, 8828−8837.
(39) Atkinson, R.; Baulch, D. L.; Cox, R. A.; Hampson, R. F., Jr.; Kerr, J. A.; Troe, J. Evaluated Kinetic and Photochemical Data for Atmospheric Chemistry Supplement IV: IUPAC Subcommittee on Gas Kinetic Data Evaluetion for Atmospheric Chemistry. *J. Phys. Chem. Ref. Data* **1992**, *21*, 1125−1568.